Collective Phenomena in the Inner Ear

- Outline
  - Background
  - Competing views of cochlear mechanics
    - * Cochlear nonlinearities mirror hair-cell nonlinearities
      - · Andronov-Hopf bifurcation
    - * Hair cells cooperate
      - · Model (invert the data)
      - · A new type of bifurcation
      - · Prediction
  - Summary

- Background
  - Anatomy & physiology
- Competing Views of Cochlear Mechanics
  - Hair-cell nonlinearities shine through
    - Eguíluz, et al., PRL, 84, 5232, 2000;

      Camalet, et al., PNAS 97, 3183, 2000.
- Andronov-Hopf bifurcation
  - What is it?
  - How is it applied to cochlear mechanics?
  - What are its predictions?
  - Are they correct?

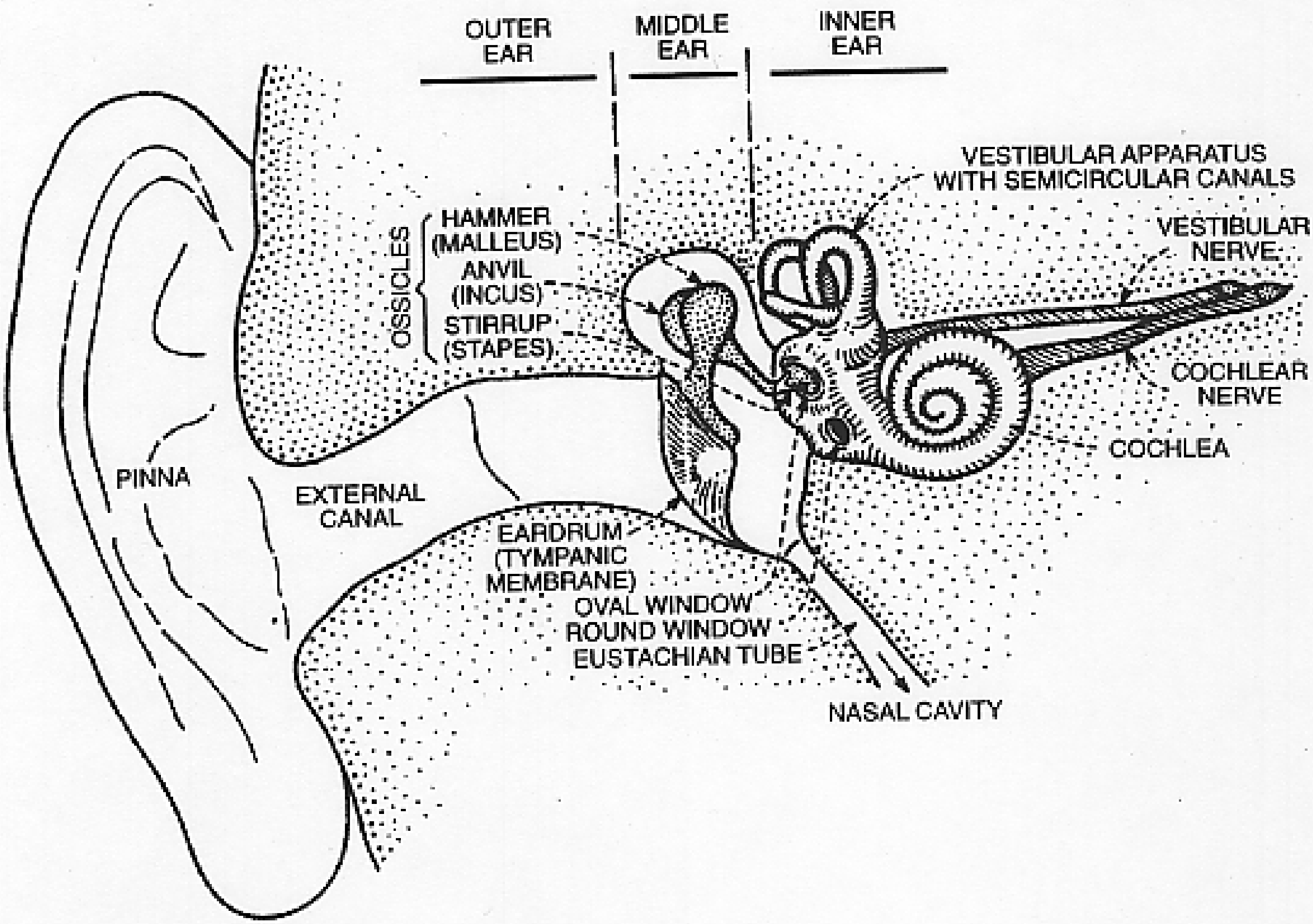
OUTER EAR
MIDDLE EAR
INNER EAR
VESTIBULAR APPARATUS WITH SEMICIRCULAR CANALS
VESTIBULAR NERVE
HAMMER (MALLEUS)
ANVIL (INCUS)
STIRRUP (STAPES)
OSSICLES
COCHLEAR NERVE
COCHLEA
PINNA
EXTERNAL CANAL
EARDRUM (TYMPANIC MEMBRANE)
OVAL WINDOW
ROUND WINDOW
EUSTACHIAN TUBE
NASAL CAVITY

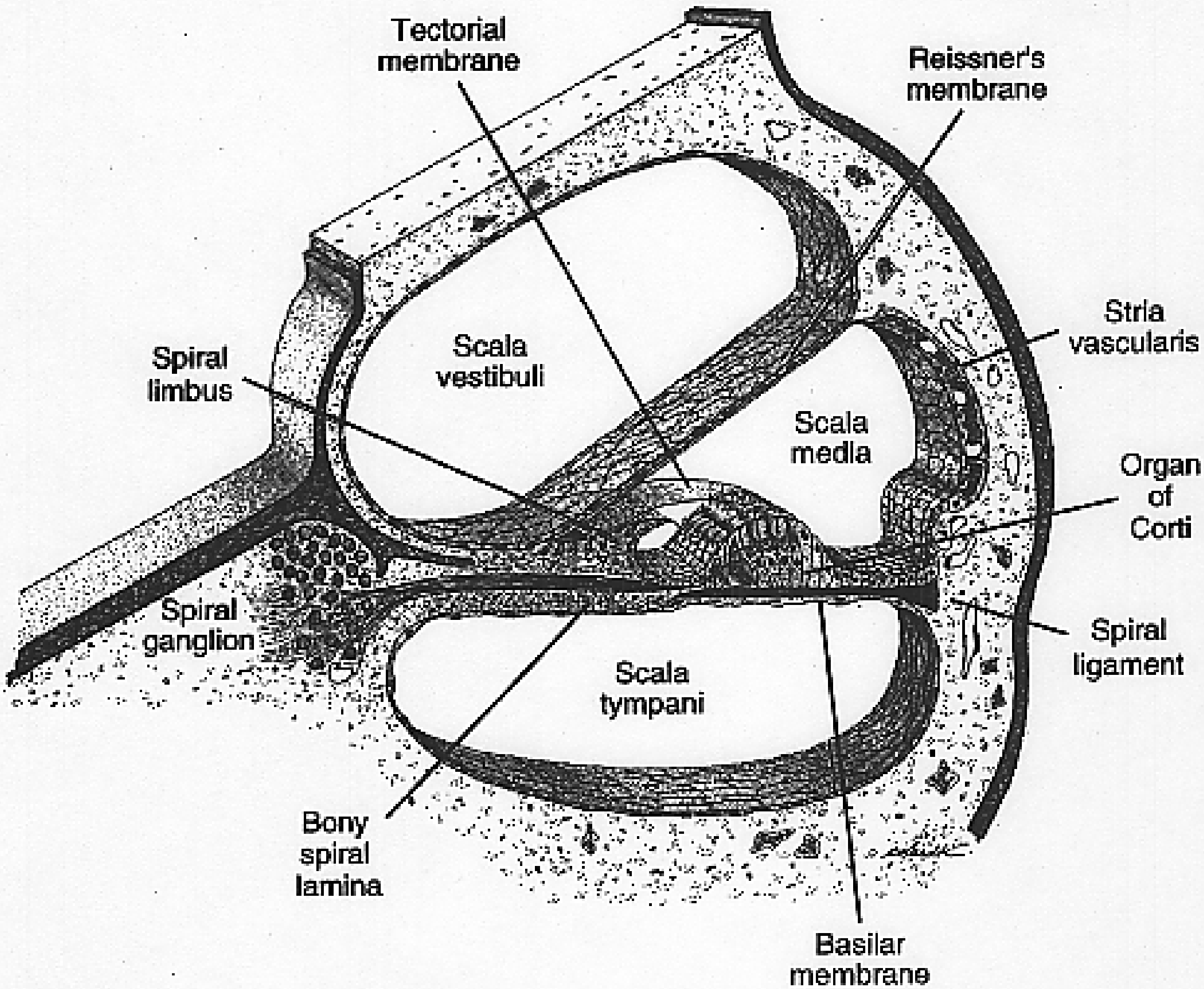
Tectorial membrane
Reissner's membrane
Stria vascularis
Scala vestibuli
Spiral limbus
Scala media
Organ of Corti
Spiral ganglion
Spiral ligament
Scala tympani
Bony spiral lamina
Basilar membrane

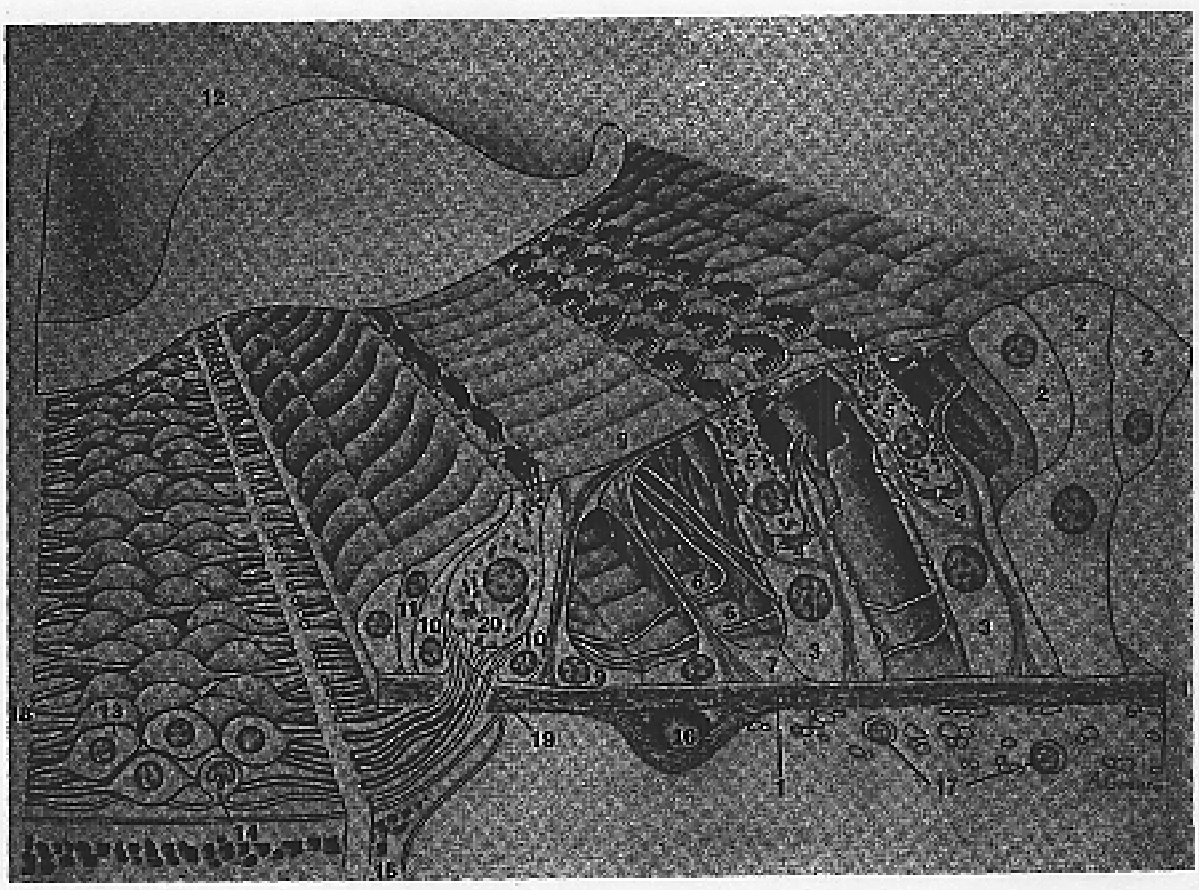

Mass on a spring with damping:

$$\ddot{x} + 2\epsilon\dot{x} + x = 0.$$

Solution:

$$x = \mathrm{e}^{-\epsilon t} \sin \omega t, \quad \omega = \sqrt{1 - \epsilon^2}$$

What if $\epsilon < 0$?

$$\ddot{x} + [2\epsilon + \mathbf{x^2}]\dot{x} + x = 0.$$

van der Pol eq.

Convention:

$$\begin{aligned} \dot{x} &= y, \\ \dot{y} &= -x - 2\epsilon y. \end{aligned}$$

Asymmetric.

$$\begin{aligned} u &= f(x, y), \\ v &= g(x, y). \end{aligned}$$

Example:

$$\begin{aligned} u &= x, \\ v &= -(y + \epsilon x)/\omega. \end{aligned}$$

$$\begin{aligned} \dot{u} &= -\epsilon u - \omega v, \\ \dot{v} &= \omega u - \epsilon v. \end{aligned}$$

In polar coordinates: $r^2 = u^2+v^2, \theta = \arctan v/u$.

$$\begin{aligned}\dot{r} &= -\epsilon r,\\ \dot{\theta} &= \omega.\end{aligned}$$

$$\begin{aligned}\dot{r} &= -(\epsilon' + ar^2)r + \cdots,\\ \dot{\theta} &= \omega' + br^2 + \cdots.\end{aligned}$$

Eguíluz, et al.:

$$\begin{aligned}\dot{r} &= -(\epsilon + r^2)r,\\ \dot{\theta} &= \omega.\end{aligned}$$

Add tone $A \sin \omega_0 t$:

$$\begin{aligned}r &\propto A^{\alpha(\omega_0)},\\ r &\propto A^{\alpha(0)} = A^1,\\ r &\propto A^{\alpha(\omega)} = A^{1/3}.\end{aligned}$$

Correct?

$$\alpha \equiv 1 - \Re\nu.$$

Andronov-Hopf bifurcation:

$$\begin{aligned}\Re\nu(\omega_0) &\leq 2/3,\\ \Re\nu(\omega) &= 2/3.\end{aligned}$$

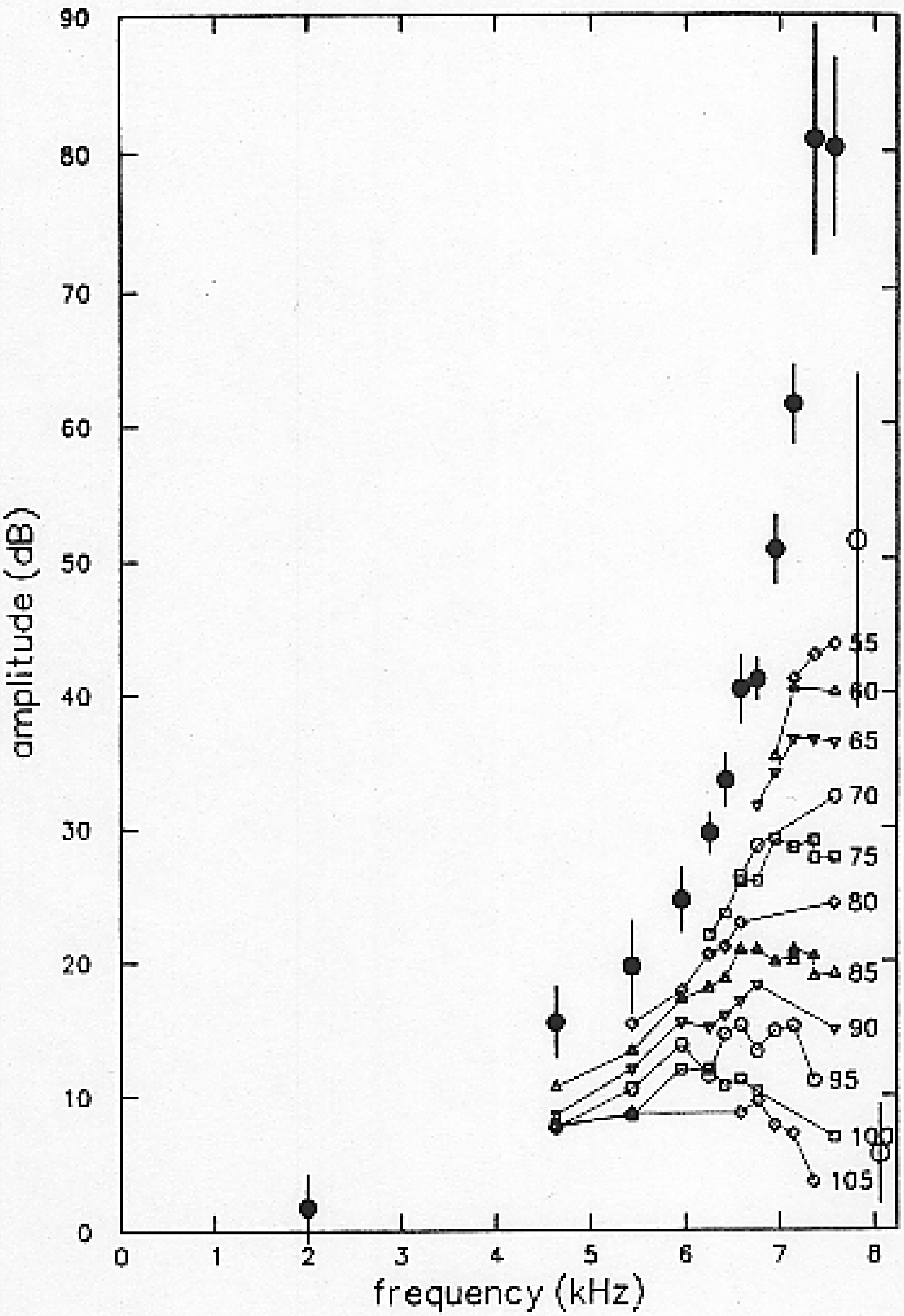

FIG. 7. Rhode's data[10] (open symbols without error flags) for the amplitude of the velocity ratio taken at constant sound-pressure level (dB values indicated) are connected by solid lines. The amplitude $|T(x,f)|$ of the transfer function found by extrapolating the velocity ratio to the constant basilar membrane displacement ($|X| = X_1 = 25$ Å) is given by the solid circles with error flags. Points above the characteristic frequency where the extrapolation is less certain are shown as open circles. Extrapolation to the constant velocity [$|V| = V_1 \approx (2\pi)7.9$ kHz (25 Å)] gives a similar result.

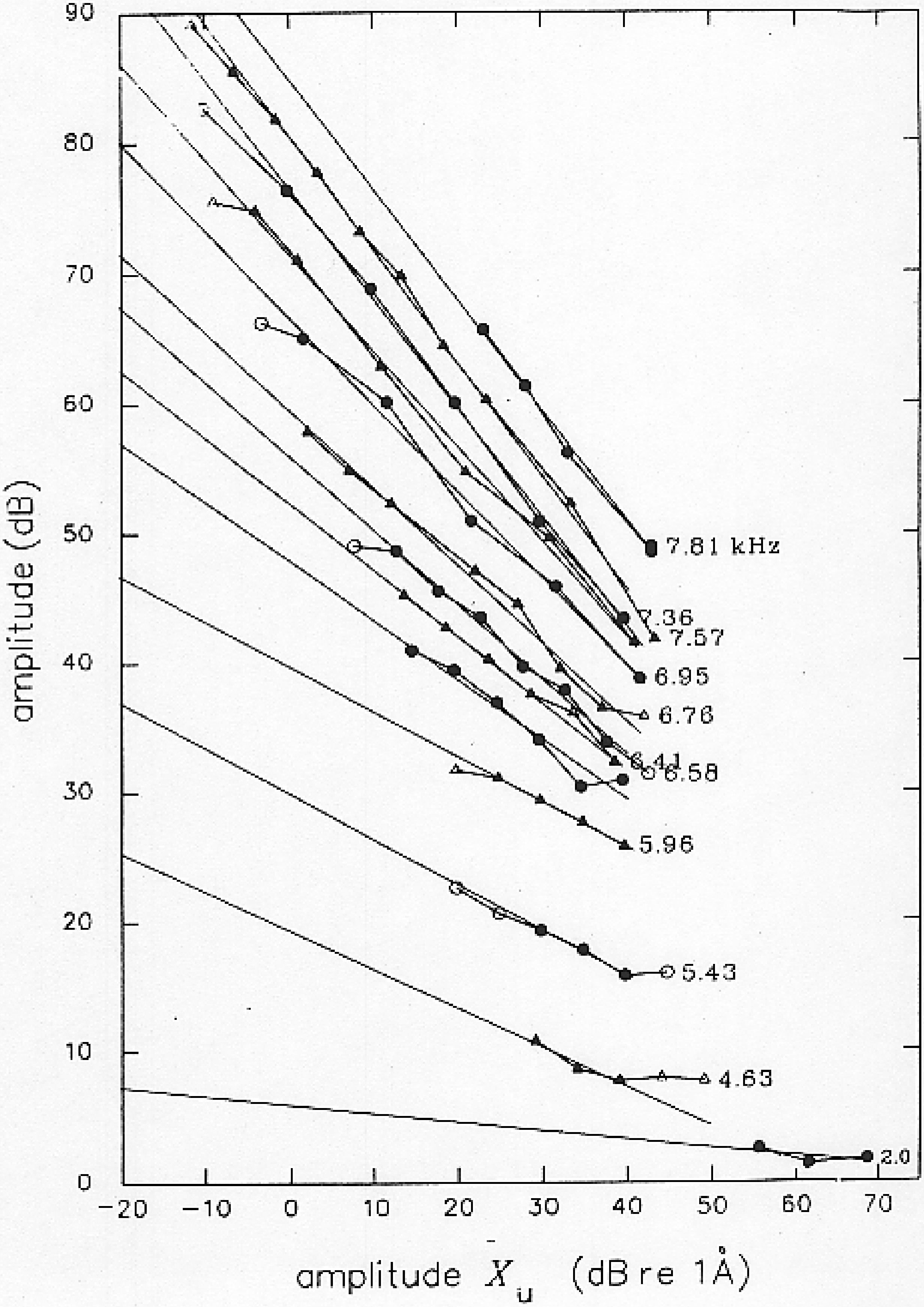

90
80
70
60
50
40
30
20
10
0
-20
-10
0
10
20
30
40
50
60
70
amplitude (dB)
amplitude $\bar{X}_u$ (dB re 1Å)
7.81 kHz
7.36
7.57
6.95
6.76
6.41
6.58
5.96
5.43
4.63
2.0

– Parameterize data:

$$D(\omega; X_u) \equiv \left[\frac{X(\omega; X_u)}{X_u}\right] \equiv \left[\frac{\tilde{X}(\omega)}{X_u}\right]^{\nu(\omega)}.$$

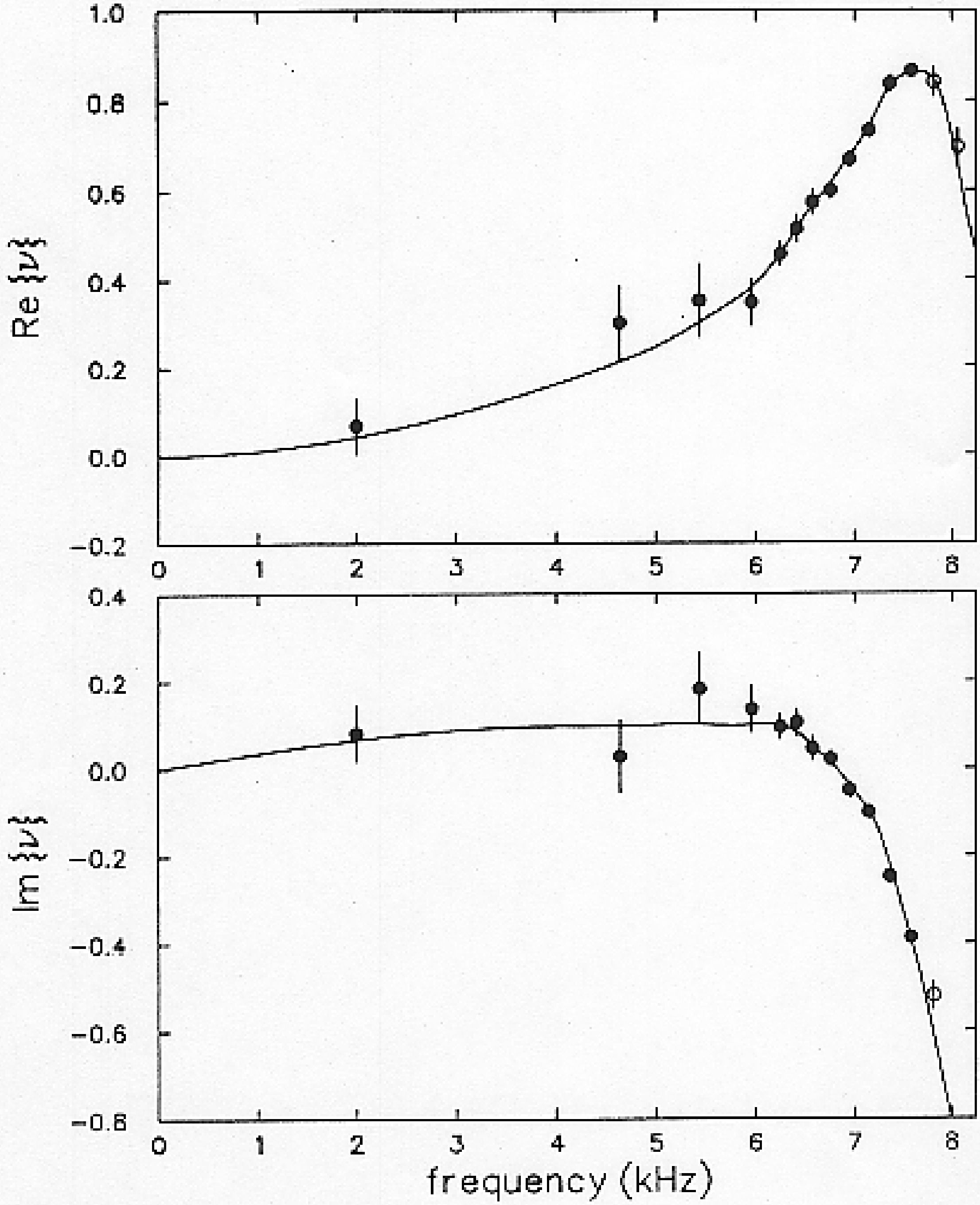

FIG. 6. The real and imaginary parts of ν plotted as a function of frequency. The two lines are a causal function fit to the data (they are Hilbert transforms of each other). The high-frequency points above the characteristic frequency are represented by open circles.

Note

$$\Re\nu(\omega) = \frac{1}{\pi} \fint_{-\infty}^{\infty} \frac{\Im\nu(\omega')}{\omega - \omega'} d\omega',$$

and,

$$\Im\nu(\omega) = -\frac{1}{\pi} \fint_{-\infty}^{\infty} \frac{\Re\nu(\omega')}{\omega - \omega'} d\omega'.$$

– $r \propto A^{1/7.5}$, not $r \propto A^{1/3}$.

- Prediction: for impulse:

$$\dot{r} = -(\epsilon + r^2) r,$$

$$r(t) = \frac{1}{\sqrt{\left(\frac{1}{r^2(0)} + \frac{1}{\epsilon}\right) e^{2\epsilon t} - \frac{1}{\epsilon}}}.$$

– Alberto Recio, N. C. Rich, S. S. Narayan, M. Ruggero: JASA 103, 1972 (1998).

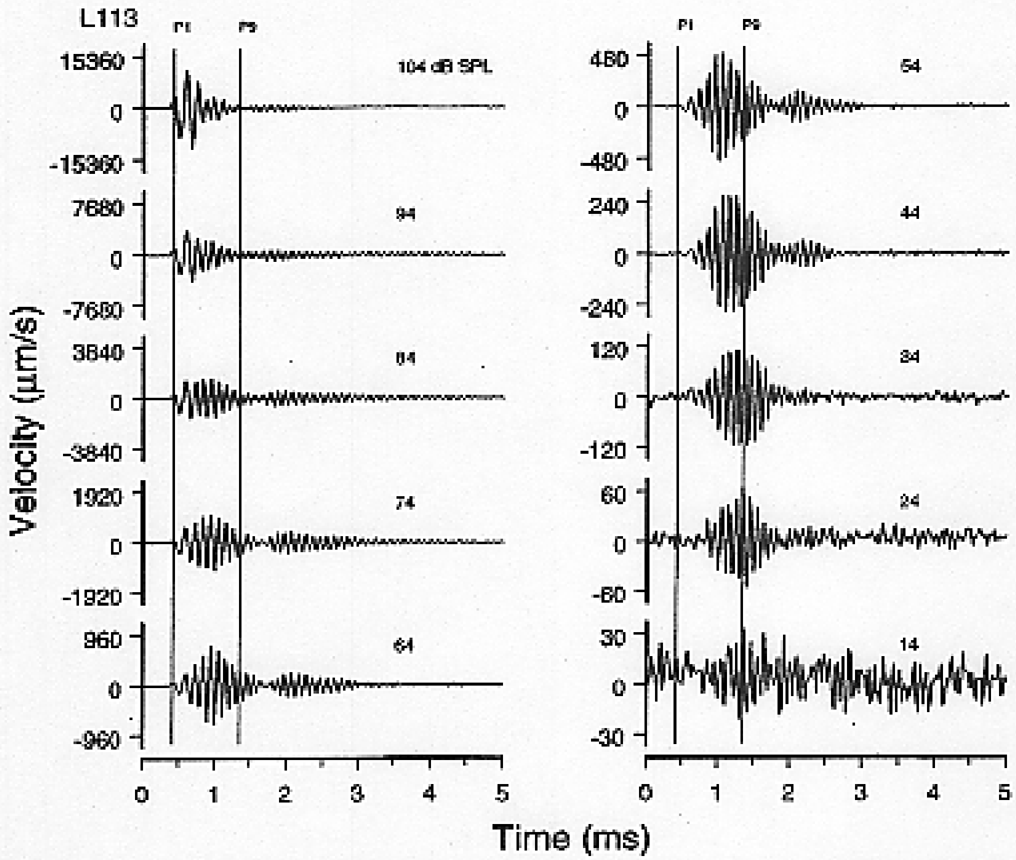

FIG. 3. Basilar-membrane responses to rarefaction clicks. The responses are displayed with scales that are systematically compressed by a ratio of 2 (i.e., 6 dB) for every increment of 10 dB in stimulus intensity. Such scaling, which de-emphasizes intensity-dependent changes in response magnitude, allows for easier comparison of the response wave shapes.

- Competing views of cochlear mechanics
  - Cochlear nonlinearities arise collectively:
- Cochlear model
  - Plan
    * Go to linear limit:

$$\lim_{X_u \to 0} D(\omega; X_u) \equiv T(\omega).$$

    * Relate T to λ.
    * Relate λ to oscillator.
    * Make oscillator nonlinear.
  - Transfer function $T = X/X_u$.
    * Independent variables:

$$\omega_c(z) \approx \omega_0 \mathrm{e}^{-z/l},$$

$$\beta \equiv \frac{\omega}{\omega_c(z)}, \quad \beta_0 \equiv \frac{\omega}{\omega_0}.$$

$$s \equiv i\beta.$$

    * Dependent variable: $T(\beta) \equiv$ displacement as a function of position.

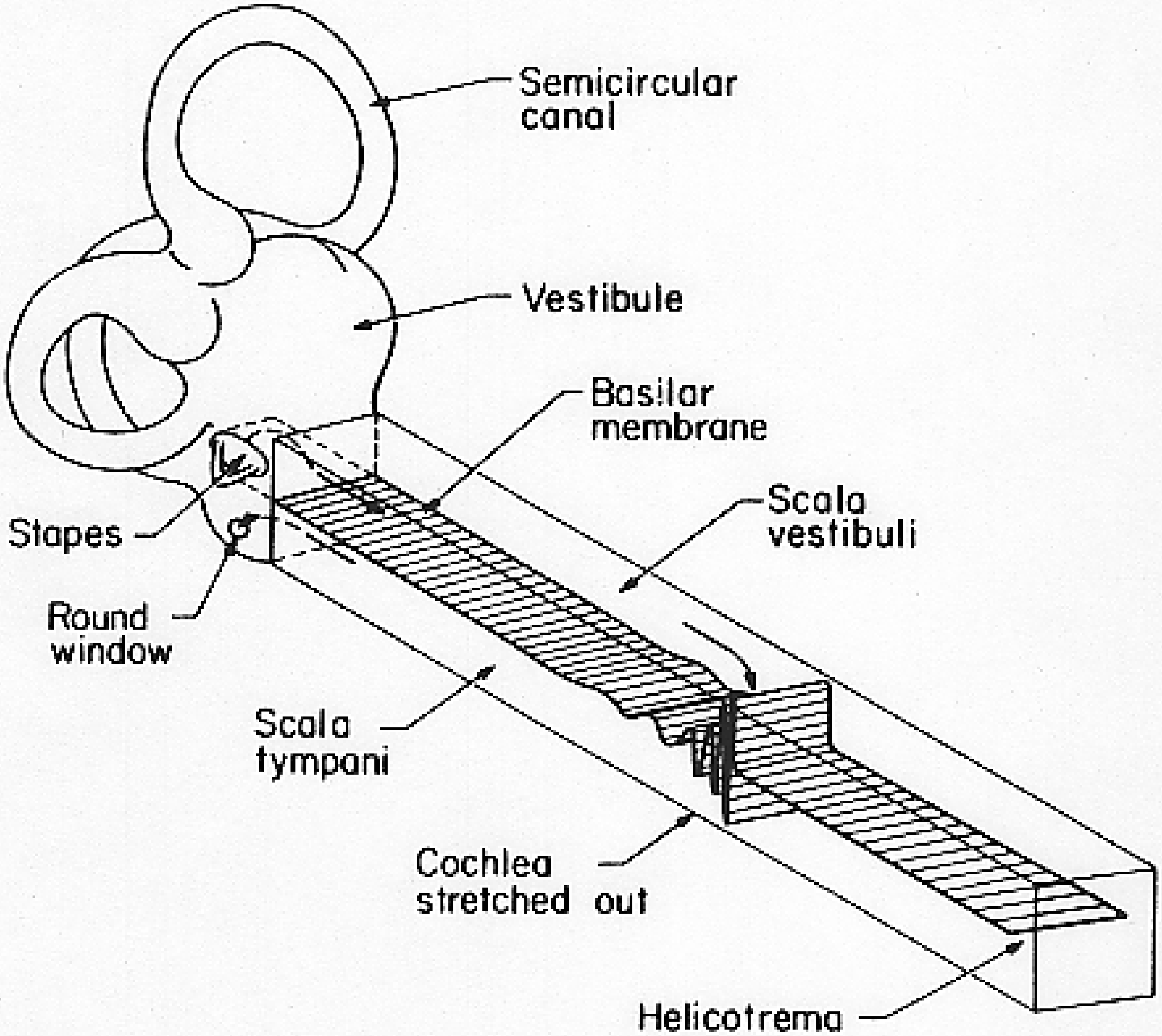

FIG. 1. Simplified model of the inner ear. The cochlea is uncoiled and approximated by two fluid-filled rigid-walled compartments (scalae vestibuli and tympani) separated by a partition (scala media, of which only the basilar membrane is shown). Sound-induced vibration of the stapes sets up a fluctuating pressure difference across the scala media, which drives its motion. The response of the basilar membrane at an instant of time to a pure tone is schematically indicated. The vertical dimensions are greatly exaggerated. The three arrows in the cochlea represent instantaneous net fluid volume velocity. When the wavelength of the wave on the basilar membrane is larger than the height of the scalae vestibuli and tympani, the region between the stapes and the helicotrema acts like a mechanical transmission line. (Reprinted, with permission, from Zweig *et al.*, Ref. 23)

– The wave:

* λ constant:

$$T \sim \mathrm{e}^{-i\left[\frac{\beta}{\lambda}+\omega t\right]}.$$

* λ slowly varying:

$$T \propto \frac{i\beta}{\lambda^{3/2}}\mathrm{e}^{-i\left[\int_{\beta_0}^{\beta}\frac{d\beta}{\lambda}+\omega t\right]}.$$

– The wavelength:

Invert: $T \longrightarrow \lambda^2$.

$$\lambda^2 \propto s^2 + 2\epsilon s + 1 + \rho \mathrm{e}^{2\pi\mu s}.$$

– The linear oscillator:

$$\ddot{x} + 2\epsilon\dot{x} + x + \rho x(t-\tau) = 0.$$

$\rho = 0$: edge of stability at $\epsilon = 0$.

$\rho \neq 0$: $\quad \epsilon = -0.09,\ \rho = 0.18,\ \tau = 2\pi\left(1\frac{3}{4}\right)$,

Good fit: $\epsilon = -0.06,\ \rho = 0.14,\ \tau = 2\pi\,(1.742)$.

– The nonlinear oscillator:

$$\ddot{x} + [2\epsilon + \sigma[\mathbf{x}^2 + \dot{\mathbf{x}}^2]]\dot{x} + x + \rho x(t-\tau) = 0.$$

Hi-fi oscillator. Combination tones are small.

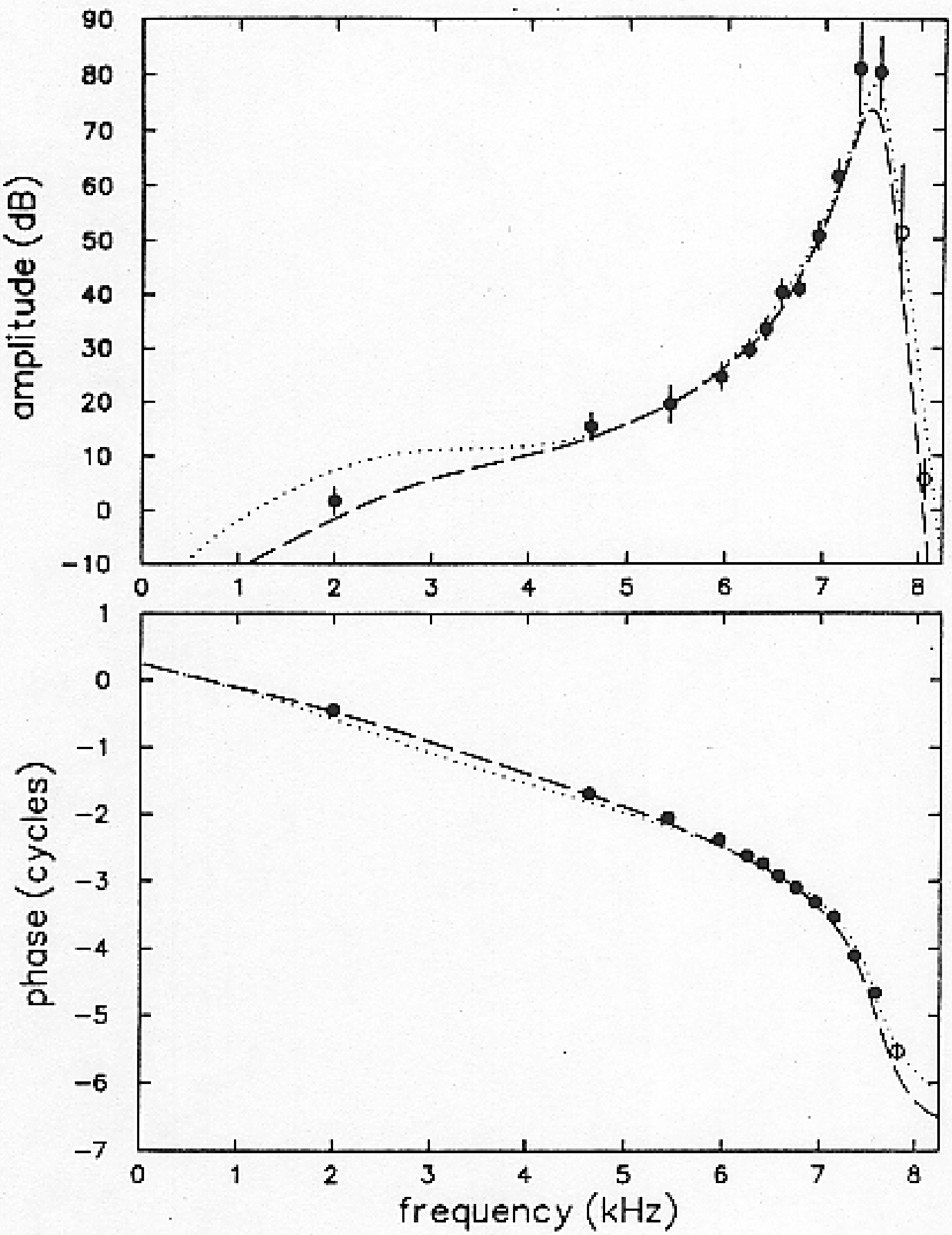

FIG. 10. The transfer function $T(x,f)$ (dashed line), derived from the empirical λ found by iteratively solving Eq. (115), is compared with extrapolated measurements (circles) of basilar membrane motion. The $T(x,f)$ corresponding to $m(s) = \rho e^{-s/\alpha}$ is shown as a dotted line. Parameter values are given in the text. The empirically determined $(4N\lambda)^2$ is shown in Fig. 11.

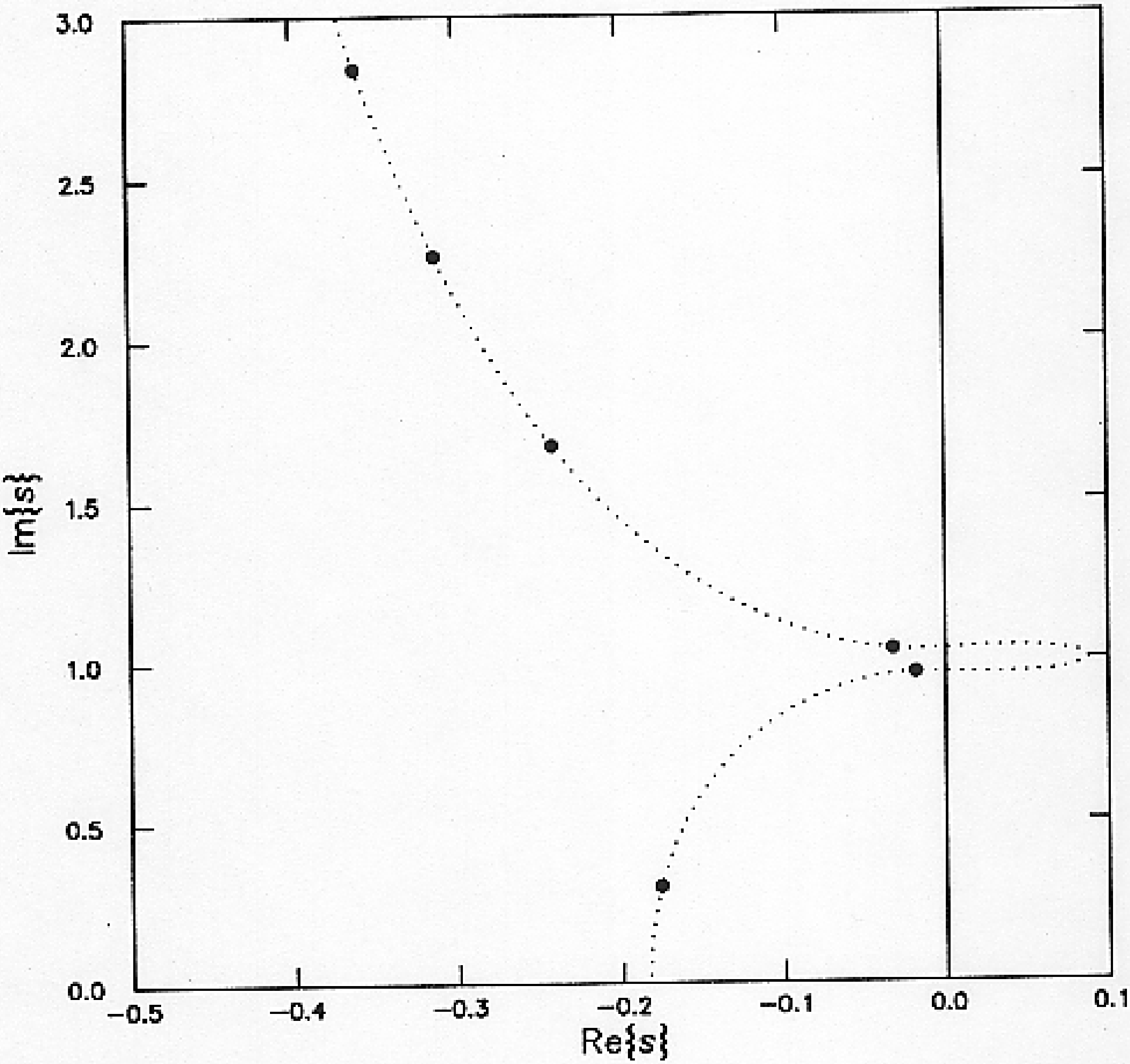

FIG. 14. The real and imaginary parts of the zeros s_n of the impedance Z in the region around $s_n = i\ [Z(s_n) = 0]$. The zeros lie on the dotted line defined by Eq. (149) and have real parts less than zero indicating that the model is stable. The two zeros near $s = i$ create the peak of the transfer function while the zero at smaller $|s|$ creates a plateau in the transfer function presumably corresponding to the "tails" of neural tuning curves.[15,71] Lowering μ from approximately $1\frac{3}{4}$ to approximately $\frac{3}{4}$ removes the zero at smaller $|s|$ and its corresponding plateau.

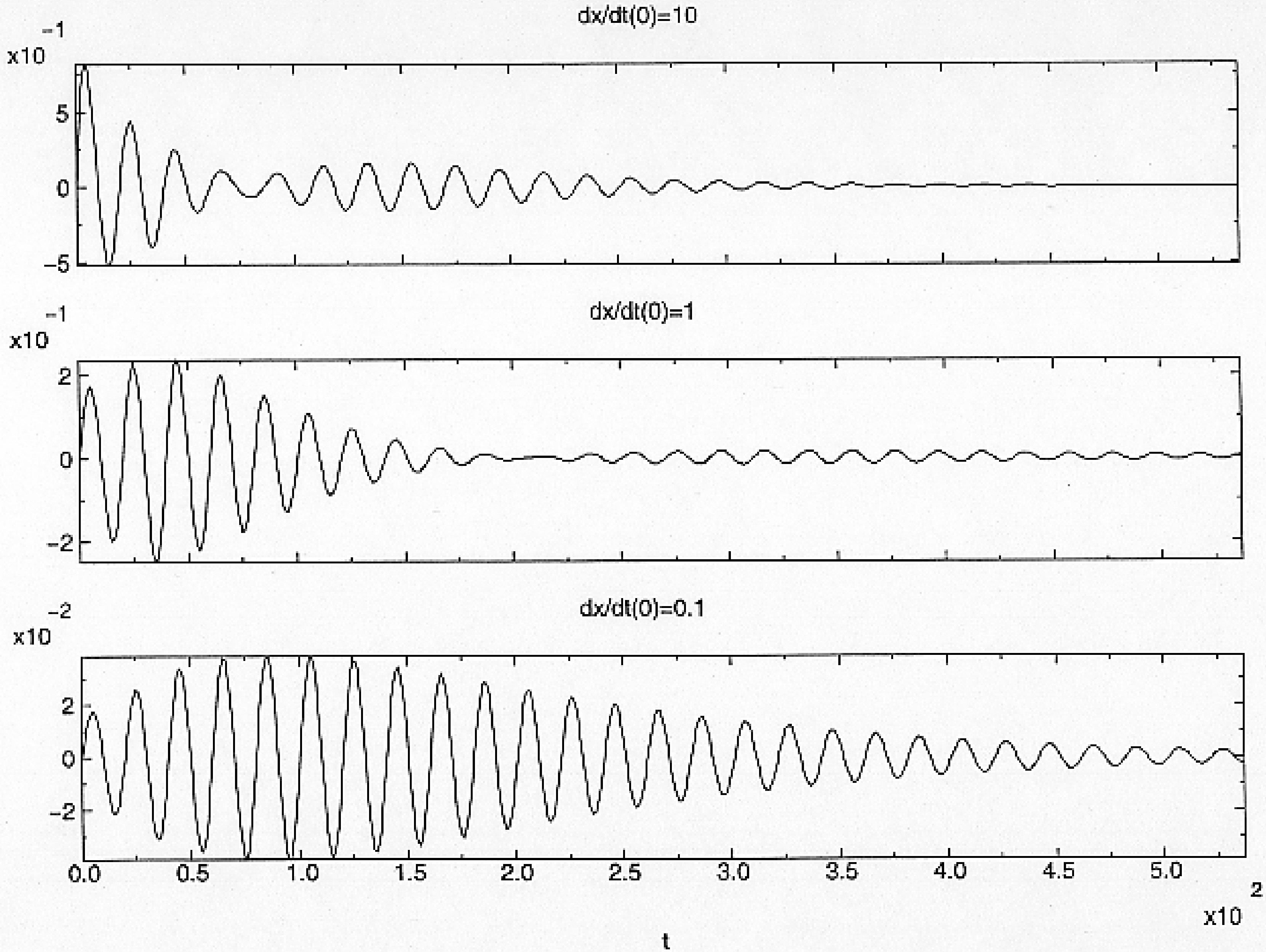
dx/dt(0)=10
x10 −1
5
0
−5
dx/dt(0)=1
x10 −1
2
0
−2
dx/dt(0)=0.1
x10 −2
2
0
−2
0.0
0.5
1.0
1.5
2.0
2.5
3.0
3.5
4.0
4.5
5.0
x10 2
t

- Interpretation:
  - 1-D fluid coupling (passive)
  - Negative damping (active)
  - Long-range stabilizing force
  - Compensation for 3-d $\longrightarrow$ 1-d
  - Nonlocality creates phase-reversal pinch

Oscillator properties:

- Active.
- Adaptive.
- Compressive.
- Harmonic distortion is negligible.
- Quiet transients long. Improves detection.
- Loud transients short. Increasing temporal resolution.
- Quiet transients have phase coherence.
  Loud transients have phase reversal.
- Zero crossings are invariant.
- Initial exponential growth. Envelope rises sharply. Accurate timing.
- The first of two pulses suppresses the second, giving a "precedence effect" (tentative).
  Reduce confusion from reverberation.
- Nonlinearities liberate oscillator from "time-frequency enslavement."
  Phase reversal $\Rightarrow$ twin peaks?
- Frequency dependent energy flow.

- Summary
  - Andronov-Hopf bifurcations are not relevant for mammalian hearing. Another type is.
  - Phase-shifting pinch in click response occurs in an isolated oscillator with time delay.
  - A simple nonlocal wave equation fits data:

$$\frac{\partial^2 d}{\partial \tau^2} - \frac{1}{\hat{\lambda}^2}\frac{\partial^2 d}{\partial t^2} = 0,$$

$$\tau(z) \equiv \frac{1}{\omega_c(z)}, \quad \hat{s} \equiv \tau(z)\frac{\partial}{\partial t},$$

$$\hat{\lambda}^2 = \lambda^2(s \rightarrow \hat{s}).$$